DEFENCE R&D DÉFENSE

A Comparison of Side-lobe Cancellation Techniques Using Auxiliary Horizontal and Vertical Antennas in HF Surface Wave Radar

Hank W.H. Leong
Defence Research Establishment Ottawa

DEFENCE RESEARCH ESTABLISHMENT OTTAWA

TECHNICAL MEMORANDUM
DREO TM 1999-121
November 1999

National Defence Défense nationale

Canada

DEFENCE R&D DÉFENSE

A Comparison of Side-lobe Cancellation Techniques Using Auxiliary Horizontal and Vertical Antennas in HF Surface Wave Radar

Hank W.H. Leong
Ground Based Radar Group
Surface Radar Section

DEFENCE RESEARCH ESTABLISHMENT OTTAWA

TECHNICAL MEMORANDUM
DREO TM 1999-121
November 1999

Project
05AB11

101-02397/

Abstract

Side-lobe cancellation techniques are evaluated using auxiliary horizontal and vertical antennas in HF surface wave radar (HFSWR). The aim of the evaluation is to compare the pros and cons of using horizontal dipoles or vertical monopoles as auxiliary antennas in HFSWR. A radar experiment was carried out to facilitate this comparison. Four horizontal dipoles, configured in the form of two separate crosses, and six vertical monopoles of a HFSWR system were used in the experiment. In this report, the central four monopoles are used as main antennas, and either two of the horizontal dipoles or the other two vertical monopoles are used as auxiliary antennas. A synthetic target signal was injected into the radar data. The effects of the cancellation techniques on the target signal are evaluated. As expected, if the target signal is coming from the same direction as the interfering signal, it is cancelled when the vertical monopoles are used as auxiliary antennas. The same target signal, however, is still visibly present when the auxiliary horizontal dipoles are used. This latter result was obtained in spite of the fact that the horizontal antennas also received the radar signal.

Résumé

Des techniques d'opposition des lobes secondaires pour des radars décamétrique à onde de surface (RDOS) sont évaluées par l'utilisation d'antennes auxiliaires verticales et horizontales. Le but de cette évaluation est de comparé les pour et les contres de l'utilisation de dipôles horizontaux ou de monopoles verticaux comme antennes auxiliaires dans un RDOS. Une expérience radar a été effectuée pour facilité la comparaison. Quatre dipôles horizontaux, arrangés en forme de deux croix séparées, et six monopoles verticaux d'un système RDOS ont été utilisés dans cette expérience. Dans ce rapport, les quatre monopoles du centre sont utilisés comme antenne principale. Les deux autres monopoles ou deux des dipôles horizontaux sont utilisés comme antennes auxiliaires. Des signaux simulé d'une cible ont été injectés dans des données radar. Les effets des techniques d'opposition des lobes secondaires sur le signal sont évalués. Comme prévu le signal de la cible est supprimé quand il vient de la même direction que l'interférence pour l'utilisation de monopoles verticaux comme antennes auxiliaires. Cependant, ce même signal est toujours visible quand on utilise plutôt des antennes horizontales. Ce dernier résultat a été obtenu en dépit du fait que les antennes horizontales recevaient aussi le signal radar.

Executive Summary

Vertically polarized antenna arrays are used in HF surface wave radar (HFSWR) to detect targets at long ranges over a sea surface beyond the line of sight. This HFSWR can be used as a cost-effective sensor for wide-area surveillance of ships and low-flying aircraft over coastal waters. The HF band is often congested with signals from communication and broadcast stations. To ensure effective and continuous operation, we must equip the radar with the capabilities of interference cancellation.

The classical side-lobe cancellation (SLC) technique [1,2] can be used to suppress the interference in HFSWR. This technique incorporates one or more auxiliary antennas into the receive system of the radar. Either horizontal or vertical antennas could be used as auxiliary antennas. In this paper, we investigate the effectiveness of the adaptive technique using auxiliary horizontal antennas, and we compare that with the effectiveness of the technique using auxiliary vertical antennas.

The investigation was carried out using a set of experiment data generated with the HFSWR at Cape Race, Newfoundland. Four horizontal dipoles, configured as two separate crosses, and six vertical monopoles of the HFSWR receive array were used. Here, we use the central four monopoles of the vertical antenna array as main antennas, and two of the horizontal dipoles or the other two monopoles as auxiliary antennas.

The results of our investigation showed that, for a target signal coming from the same direction as the interfering signal, both the interfering and target signals were cancelled when the vertical monopoles were used as auxiliary antennas. However, the target signal was preserved while the interference was cancelled when the horizontal dipoles were used as auxiliary antennas.

The cancellation of targets from the same direction as the interfering signal, when auxiliary vertical antennas were used, could lead to a failure to detect targets close to the interference direction. This failure, however, could be avoided if we use horizontal antennas such as horizontal dipoles as auxiliary antennas in the SLC system.

The results above were obtained using a synthesised target signal injected into measured radar data. To further verify the results above, it is recommended that we carry out a similar experiment with a real target signal in the radar data.

Leong, Hank W. H., A Comparison of Side-lobe Cancellation Techniques Using Auxiliary Horizontal and Vertical Antennas in HF Surface Wave Radar, Defence Research Establishment Ottawa, DREO TM 1999-121, November 1999.

Sommaire

Des réseaux d'antenne polarisée verticalement sont utilisés dans les radars décamétrique à onde de surface (RDOS). Ces radars sont utilisés pour la détection des cibles éloignées volant au-dessus de l'océan au-delà de la portée optique. Ces RDOSs peuvent être utilisés comme des détecteurs relativement peu coûteux pour la surveillance des navires et des avions volant à basse altitude dans les eaux littorale et sur de grandes couvertures. La bande HF est souvent congestionnée avec des signaux de communication radios et des stations de diffusions. Pour s'assurer des opérations continue et effective, nous devons équiper les radars avec la capacité d'annuler les interférences.

Les techniques classiques d'annulation des lobes latéraux (SLC) peuvent être utilisés pour réduire les interférences dans les RDOS. Ces techniques incorpore une ou plusieurs antenne auxiliaire dans le système de réception du radar. Des antennes verticales ou horizontales peuvent être utilisées comme antennes auxiliaires. Dans ce rapport, nous étudions l'efficacité des techniques adaptatives utilisant des antennes horizontales auxiliaires, et nous comparons cela avec l'efficacité des techniques utilisant des antennes auxiliaire verticales.

Les recherches ont été effectuées en utilisant un ensemble de données expérimentales généré avec le RDOS situé à Cap Race, Terre Neuve. Quatre dipôles horizontaux disposés comme 2 croix séparées, et 6 monopoles verticaux du réseau de réception du RDOS ont été utilisés. Les quatre monopole centrales du réseau d'antenne verticale sont utilisé comme antenne principales, et deux des dipôles horizontales (ou les deux autres monopole) comme antenne auxiliaires.

Les résultats de nos recherches montrent que, pour un signal venant de la même direction que l'interférence, les signaux de l'interférence et de la cible sont les tous les deux annulés quand les monopoles verticaux sont utilisés comme antennes auxiliaires. Cependant, le signal de la cible est préservé et l'interférence annulée quand des dipôles horizontaux sont utilisés comme antennes auxiliaires.

L'annulation des signaux de cibles provenant de la même direction que l'interférence, quand les antennes verticales auxiliaires sont utilisées, peut conduire à l'incapacité de détecter des cibles proche de cette direction d'interférence. Ce problème, cependant, peut être éviter si nous utilisons

des antennes horizontales tel que des dipôles horizontaux auxiliaires dans les systèmes d'annulation des lobes latéraux.

Les résultats ci dessus ont été obtenus en injectant un signal synthétique de cible dans les données radar. Pour vérifier en profondeur les résultats précédants, il est recommandé que nous effectuons des expériences similaires en utilisant des signaux de cible réelle dans les données radar.

Leong, Hank W. H., A Comparison of Side-lobe Cancellation Techniques Using Auxiliary Horizontal and Vertical Antennas in HF Surface Wave Radar, Defence Research Establishment Ottawa, DREO TM 1999-121, November 1999.

Table of Contents

Abstract iii

Résumé iv

Executive Summary v

Sommaire vii

Table of Contents ix

List of Figures xi

1. Introduction 1

2. Side-Lobe Cancellation Techniques 1

3. Experimental Radar Data 6

   3.1 Doppler Spectra of Array Element Outputs 7

   3.2 Doppler Spectra of Beamformed Outputs from Main Array 10

4. Results of Interference Suppression 15

   4.1 Target signal coming from the same direction as the interfering signal 16

   4.2 Effects of Interference Suppression on Sea Clutter and Interference-plus-Noise Power Spectral Densities 20

   4.3 Implications of Experimental Results 23

5. Conclusions and Recommendations 24

Acknowledgements 24

Reference 25

List of Figures

Figure 1 Configuration of side-lobe cancellation system 2

Figure 2 Receiving antenna configuration (top view) 7

Figure 3 Power spectral densities of outputs from auxiliary antennas at the specified range bin of 27; (a)-(d) -- horizontal dipoles; (e)-(f) -- vertical monopoles 9

Figure 4 Power spectral densities of outputs from auxiliary antennas at the specified range bin of 15; (a)-(d) -- horizontal dipoles; (e)-(f) -- vertical monopoles 11

Figure 5 Power spectral densities of outputs from main antennas (vertical monopoles 6, 7, 8 and 9) at the specified range bin of 27 12

Figure 6 Power spectral densities of outputs from main antennas (vertical monopoles 6, 7, 8 and 9) at the specified range bin of 15 13

Figure 7 Power spectral densities of beamformed outputs from main array at the specified range bin of 27 14

Figure 8 Power spectral densities before interference Suppression (a), after interference suppression with auxiliary horizontal dipoles 1 and 2 (b), after interference suppression with auxiliary horizontal dipoles 3 and 4 (c), and after interference suppression with auxiliary vertical monopoles 5 and 10 (d); The target Doppler frequency is at 2 Hz. 17

Figure 9 Power spectral densities before interference Suppression (a), after interference suppression with auxiliary horizontal dipoles 1 and 2 (b), after interference suppression with auxiliary horizontal dipoles 3 and 4 (c), and after interference suppression with auxiliary vertical monopoles 5 and 10 (d); The target Doppler frequency is at –0.132 Hz. 19

Figure 10 Superimposed Doppler spectra of outputs from beam No. 1 before and after interference suppression 21

Figure 11 Superimposed Doppler spectra of outputs from beam No. 2 before and after interference suppression 22

Figure 12 Superimposed Doppler spectra of outputs from beam No. 3 before and after interference suppression 22
Figure 13 Superimposed Doppler spectra of outputs from beam No. 4 before and after interference suppression 23

1. Introduction

A high-frequency surface-wave radar (HFSWR) utilises the surface-wave mode of electromagnetic wave propagation over sea water to detect targets (e.g., ships and aircraft) at distances beyond the line of sight. The radar is a cost-effective sensor for wide-area surveillance of coastal waters at distances up to 450 km for ships and up to 180 km for low level aircraft. To detect ship and aircraft targets, the HFSWR is usually operated in the lower end of the high frequency band (e.g., 2-15 MHz). One problem encountered in the operation of the radar in this frequency band is that of night-time interference propagated via the skywave mode from the other users of the same frequency band. Ionospheric conditions at night favour the propagation of the radio signals over very long distances. This effectively increases the number of interfering signals at a given radar site, and makes it sometimes impossible to find a clear channel to operate the radar.

The classical side-lobe cancellation (SLC) technique [1,2] can be used to suppress the interference in HFSWR. Either horizontal or vertical antennas could be used as auxiliary antennas in the SLC system. The HFSWR employs vertically polarized transmit and receive antennas for long range target detection. Here, it is shown that

(1) If vertical antennas are used as auxiliary antennas, the radar cannot detect targets close to the directions of the interfering signals.

(2) If horizontal antennas are used as auxiliary antennas, the radar can detect targets arbitrarily close to the directions of the interfering signals.

2. Side-Lobe Cancellation Techniques

Figure 1 shows a configuration of the adaptive SLC system. The SLC system incorporates one or more auxiliary antennas into the receive system of the radar. The outputs of the auxiliary antennas are correlated with the outputs of the main antennas. From this correlation, we estimate

a set of weight vectors for the outputs of the auxiliary antennas. The sums of the weighted outputs from the auxiliary antennas represent estimates of the interference components in the outputs of the main antennas. A subtraction of the estimates from the outputs of the main antennas then results in a suppression of the interference.

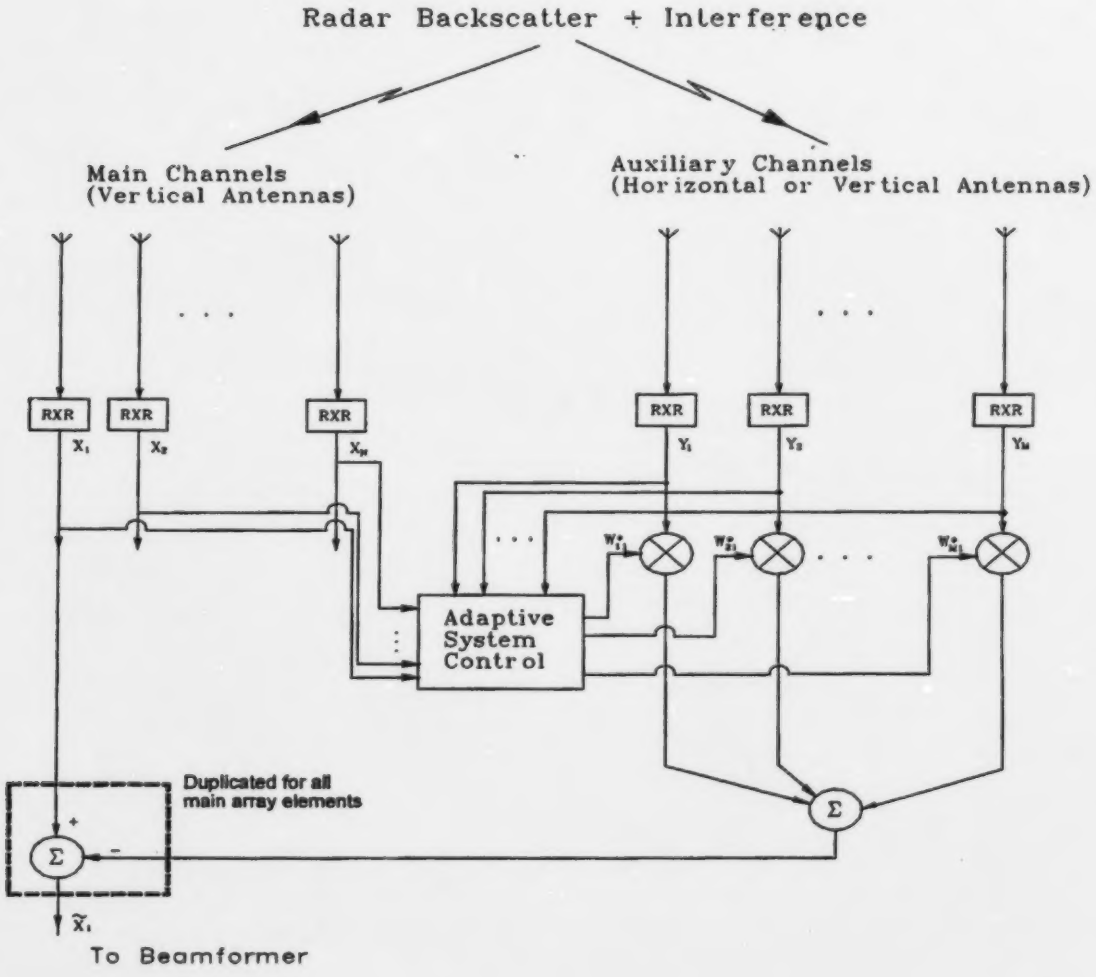

Figure 1 Configuration of side-lobe cancellation system

The inputs to the SLC system in Figure 1 are defined as:

$\mathbf{x}$ = a snapshot of the outputs of the main antennas at a specified range bin
$= (x_1, x_2, \ldots, x_N)^T$

$\mathbf{y}$ = a snapshot of the outputs of the auxiliary antennas at the same range bin
$= (y_1, y_2, \ldots, y_M)^T$

Here we assume that the SLC system has a total of N main channels and a total of M auxiliary channels.

Define a set of complex weight vectors, $\mathbf{w}_n$, as $\mathbf{w}_n = (w_{1n}, w_{2n}, \ldots, w_{Mn})^T$, n=1,2, …, N. The output complex amplitudes of the adaptive system is given by

$$\tilde{\mathbf{x}} = \mathbf{x} - \mathbf{W}^H \mathbf{y} \tag{1}$$

where $\tilde{\mathbf{x}} = (\tilde{x}_1, \tilde{x}_2, \ldots, \tilde{x}_N)^T$ and $\mathbf{W} = (\mathbf{w}_1, \mathbf{w}_2, \ldots, \mathbf{w}_N)$.

The output power of the system is given by

$$P = E[\,|\tilde{\mathbf{x}}|^2\,] = E[\,|\mathbf{x} - \mathbf{W}^H \mathbf{y}|^2\,] \tag{2}$$

where $\mathbf{W}^H$ is the conjugate transpose of $\mathbf{W}$.

For interference suppression, the output power P is minimized with respect to the real and imaginary parts of the weights, w_{mn}, for m=1,2, …, M and n=1,2, …, N. From this minimization, we obtain an optimal weight matrix, $\mathbf{W}_{opt}$, in a form of the Wiener solution [3]:

$$\mathbf{W}_{opt} = \mathbf{R}_{yy}^{-1} \mathbf{R}_{yx} \tag{3}$$

where $\mathbf{R}_{yy}^{-1}$ is the inverse of the covariance matrix of the outputs from the auxiliary antennas, and $\mathbf{R}_{yx}$ is the cross-correlation matrix between the outputs of the auxiliary antennas and the outputs of the main antennas.

The optimal weight matrix $\mathbf{W}_{opt}$ is substituted into Equation (1) to cancel the interference. The second term in Equation (1), $\mathbf{W}^H\mathbf{y}$, represents an estimate of the interference components in the outputs of the main array. By subtracting this estimate from the outputs of the main array, we then cancel the interference at the output of the SLC system.

The purpose of the auxiliaries is to provide replicas of interfering signals for cancellation [2]. Here, the side-lobe cancellation is not only in the spatial domain, but also in the polarization domain. If the type of auxiliaries is the same as that of the main antennas (e.g., both being vertical monopoles), then the auxiliaries see the target and interfering signals no different from the main antennas. Therefore, the SLC system has no capability to distinguish the target signal from the interfering signal when the target signal is coming from the same direction as the interfering signal. However, if the polarization of the auxiliaries is different from that of the main antennas (e.g., auxiliaries being horizontal dipoles and main antennas being vertical monopoles), then the auxiliaries may see the target and interfering signals differently, provided that there is a difference in the polarizations of the target and interfering signals. Therefore, in this case, it is possible for the SLC system to distinguish the target signal from the interfering signal even when the target and interfering signals are coming from the same direction. In the following, we illustrate, using a simple signal model, how the SLC system using the auxiliary horizontal dipoles can cancel the interference without cancelling the vertically polarized target signal in HFSWR.

Let $\mathbf{s}_m$ and $\mathbf{s}_a$ be respectively the target signals received by the main and auxiliary arrays, and $\mathbf{r}_m$ and $\mathbf{r}_a$ be the interference components received by the same arrays. The outputs received by the main and auxiliary arrays can be expressed by

$$\mathbf{x} = \mathbf{s}_m + \mathbf{r}_m \tag{4}$$

$$\mathbf{y} = \mathbf{s}_a + \mathbf{r}_a \tag{5}$$

Here, we neglect the noise components received by the main and auxiliary arrays. In the presence

of interference, the noise components are considerably smaller than the interference components.

In theory, the horizontal dipoles do not receive the vertically polarized target signal. Therefore, if horizontal dipoles are used as auxiliary antennas, we have that $\mathbf{s}_a = \mathbf{0}$ and consequently, $\mathbf{y} = \mathbf{r}_a$. The output of the adaptive system can then be written as

$$\tilde{\mathbf{x}} = \mathbf{s}_m + (\mathbf{r}_m - \mathbf{W}^H \mathbf{r}_a) \tag{6}$$

and the output power P is given by

$$P = E\left[\left| \mathbf{s}_m + (\mathbf{r}_m - \mathbf{W}^H \mathbf{r}_a) \right|^2 \right] \tag{7}$$

If the radar signal and the interfering signal are not correlated, then the output power of the system can be further simplified as

$$P = E[|\mathbf{s}_m|^2] + E[|\mathbf{r}_m - \mathbf{W}^H \mathbf{r}_a|^2] \tag{8}$$

Equation (8) shows that by minimizing the output power P, we minimize the power of the interference in the output of the adaptive system. The first term on the right-hand side of Equation (8) represents the power of the received target signal in the main array. This term remains unchanged throughout the minimization process. Hence, by minimizing the power of the interference, we maximize the signal-to-interference-plus-noise density ratio (SINR) in the output of the SLC system.

In practice, the horizontal dipoles could receive the target signal, often due to an imperfect alignment of the dipoles. In this report, we show, by experimental results, that the SLC system using the auxiliary dipoles could still suppress the interference without cancelling the target signal, even when the target signal is coming from the same direction as the interference.

Implementation of Adaptive Algorithm

We use the array snapshots at long ranges to estimate the correlation matrices, $\mathbf{R}_{yy}$ and $\mathbf{R}_{yx}$. Let K_m be the range bin corresponding to the maximum range, or close to the maximum range, of the radar, and K_n be the number of range bins used to estimate $\mathbf{R}_{yy}$ and $\mathbf{R}_{yx}$. For each waveform repetition interval (WRI), we calculate the estimates of $\mathbf{R}_{yy}$ and $\mathbf{R}_{yx}$ with

$$\tilde{\mathbf{R}}_{yy} = \frac{1}{N} \sum_{k=K_m-K_n+1}^{K_m} \mathbf{y}_k \mathbf{y}_k^H \tag{9}$$

and

$$\tilde{\mathbf{R}}_{yx} = \frac{1}{N} \sum_{k=K_m-K_n+1}^{K_m} \mathbf{y}_k \mathbf{x}_k^H \tag{10}$$

where $\mathbf{x}_k$ and $\mathbf{y}_k$ represent a snapshot of the main and auxiliary antenna outputs at range bin k. For the current set of radar data, we arbitrarily set K_m=240 and K_n=60. For each WRI, we use the estimates of $\mathbf{R}_{yy}$ and $\mathbf{R}_{yx}$ in Equation (3) to compute the weight matrix $\mathbf{W}_{opt}$. The snapshot samples $\mathbf{x}_k$ and $\mathbf{y}_k$ in Equations (4) and (5) could be obtained from either the previous WRI or the current WRI. In this report, we use the samples from the previous WRI for the estimation of $\mathbf{W}_{opt}$.

3. Experimental Radar Data

The set of experimental data was collected with the HFSWR at Cape Race, Newfoundland. Four horizontal dipoles, configured as two separate crosses, and six vertical monopoles of the HFSWR receive array were used in the experiment. Figure 2 shows a top view of the receiving antenna configuration. Here, we number the four horizontal dipoles as elements 1-4 and the six monopoles as elements 5-10. The vertical antenna array was aligned with the coastline at Cape Race. The array was linear and uniform, and had an element spacing of 22.2 m. The horizontal dipoles were located behind the vertical antenna array. In this report, we use the central four monopoles (element numbers 6, 7, 8 and 9) as main antennas, and we use two of the horizontal

dipoles or two monopoles as auxiliary antennas.

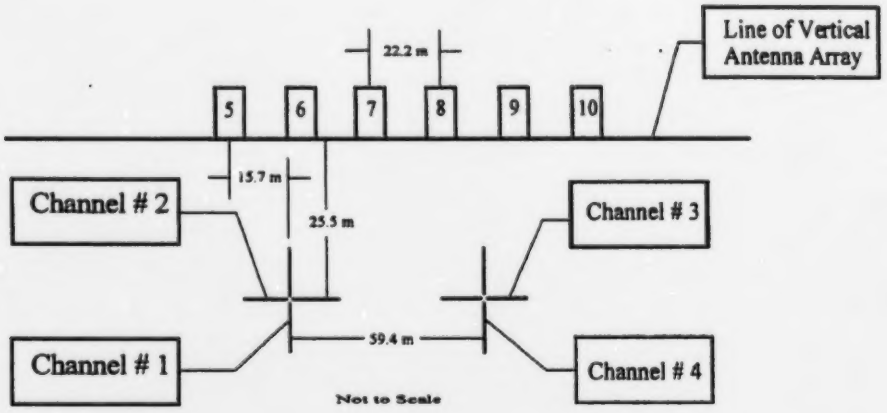

Figure 2 Receiving antenna configuration (top view)

The HFSWR system operated at a nominal frequency of 5.811 MHz, using a frequency-modulated-interrupted-waveform (FMICW). The swept bandwidth of the waveform was 125 kHz and the waveform repetition frequency (WRF) was 9.01 Hz. Correspondingly, the waveform repetition interval of the radar was 110 milli-seconds.

The radar experiment was carried out at night when there was strong interference. The radar operated from 02:22:44 AM to 03:10:05 AM, local time, on 29 March 1995. The collected data consisted of 256 range bin samples. The range resolution of the radar was 1.2 km, and the first range bin of the radar was centred at 2 km. Hence, the received data represented the radar echoes from the ranges between 2 and 308 km. After the data collection, a preliminary processing was carried out to equalize the gain and phase responses of the array elements.

3.1 Doppler Spectra of Array Element Outputs

At each range bin, a time series of the radar echoes from each array element can be formed over consecutive WRIs. A power spectral density (PSD) of the time series can then be computed

by using the Fast Fourier Transform (FFT). For the current set of data, we use a 1024-point FFT. To reduce the leakage of power outside the signal frequency bin, we use a Blackman window [5] before the application of the FFT. At the WRF of 9.01 Hz, the coherent integration time (CIT) is 1.89 minutes. To minimize the fluctuation of the FFT outputs, we sum the power spectral density at each frequency bin over all the spectra of non-overlapping time series available from the radar data. There are 24 power spectra available. Hence, the duration over which we sum the power of the FFT outputs is equal to 45.5 minutes. Figures 3 shows, respectively, the integrated spectral outputs of the auxiliary antennas that we use in this report, namely, the horizontal dipole elements 1, 2, 3 and 4, and the vertical monopole elements 5 and 10. The range bins for the spectra are all equal to 27. This corresponds to a range centred at 33.2 km. Figure 3 shows that there is a small peak at the Doppler frequency of about –0.3 Hz in the PSDs of the time series, due to the interference present at the outputs of the auxiliary antennas.

The PSDs of the time series for the vertical antennas include two spectral lines, referred to as Bragg lines, representing the first-order sea echoes of the radar [4]. These two spectral lines are the result of a resonant scattering of the radar signal by the approaching and receding ocean waves that have a wavelength equal to one half of the radar wavelength. In the absence of ocean currents, the Bragg lines have unique Doppler frequencies [4] at

$$f_B = \pm\sqrt{\frac{g}{\pi\lambda}} \tag{11}$$

where g is the gravitational acceleration ($g = 9.81$ m/s^2) and λ is the radar wavelength ($\lambda = c/f$, where c is the speed of light and f the radar frequency). Note that the "+" and "-" signs in Equation (6) indicate that the Bragg lines are scattered back, respectively, by the approaching and receding ocean waves. At the radar frequency of 5.811 MHz, the radar wavelength is 51.63 m, and the frequencies of the Bragg lines are ±0.246 Hz. In the absence of interference, the Bragg lines are usually very strong in the PSD of the time series. During daytime, for example, the Bragg lines can be at tens of decibels above the background noise. However, because of the interference, the Bragg lines are barely observable in Figures 3(e) and 3(f).

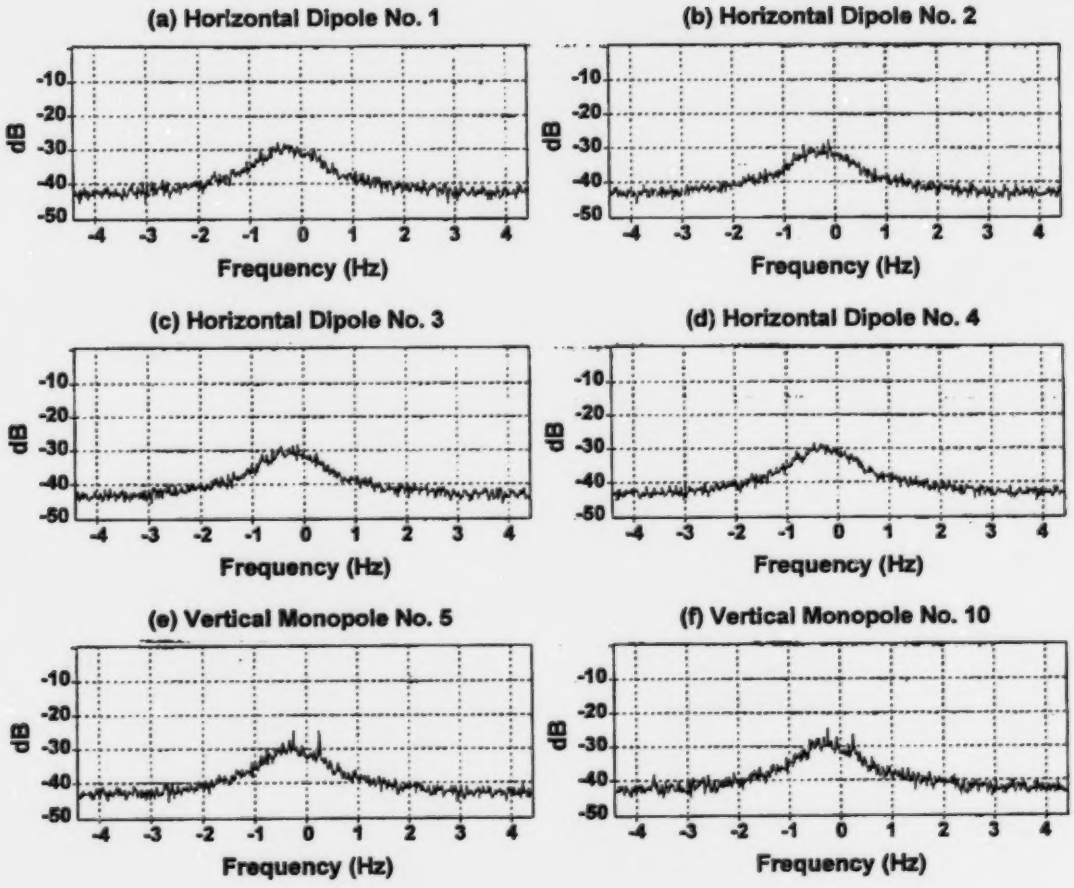

Figure 3 Power spectral densities of outputs from auxiliary antennas at the specified range bin of 27; (a)-(d) -- horizontal dipoles; (e)-(f) -- vertical monopoles

Figure 4 shows the integrated spectra of the same antenna outputs for the range bin of 15, which corresponds to a range centred at 18.8 km. At this closer range bin, the Bragg lines are now clearly observable, from both the PSDs for the vertical antennas and for the horizontal antennas. Figure 4 shows that while the interference-plus-noise levels are about the same in the PSDs of the time series, the Bragg lines in the outputs of the horizontal antennas are about 6-8 dB lower than those in the outputs of the vertical antennas. Hence, the signal amplitudes of the Bragg lines from the horizontal antennas are about 40%-50% of the signal amplitudes of the Bragg lines from the vertical antennas.

The outputs of the main antennas (i.e., elements 6,7,8 and 9) are similar to the outputs of vertical monopoles 5 and 10. Figures 5 and 6 show the integrated spectra of the main antennas for the specified range bins of 27 and 15, respectively. Again, the interference could be observed from all the spectra. While the Bragg lines are barely observable at the range bin of 27, the Bragg lines are only about 14-15 dB above the interference-plus-noise levels at the range bin of 15.

3.2 Doppler Spectra of Beamformed Outputs from Main Array

Beamforming of the outputs from the main array can be carried out by using the FFT algorithm. The beamformed outputs can then be Doppler-processed by using the procedure described in Section 3.1. The azimuth angle of the FFT amplitude in the directional spectrum is given by $\theta_i = \sin^{-1}(\frac{i\lambda}{nd})$, where i is the bin number of a n-point FFT and i ranges from -n/2 to n/2-1. Here, we use a four-point FFT for the four-element array. Figure 7 shows the Doppler spectra of the outputs from the beams formed by using the FFT. In the spectrum of the outputs from the main beam along the boresight of the main array (Beam No. 1), the interference dominates over the sea clutter and the Bragg lines cannot be observed from the spectrum. In the spectra of the outputs from the other beams (Beam No. 2, 3 and 4), the interference is less severe and the Bragg lines are clearly visible. Figure 7 shows that the interference is mainly coming from the boresight direction of the main array.

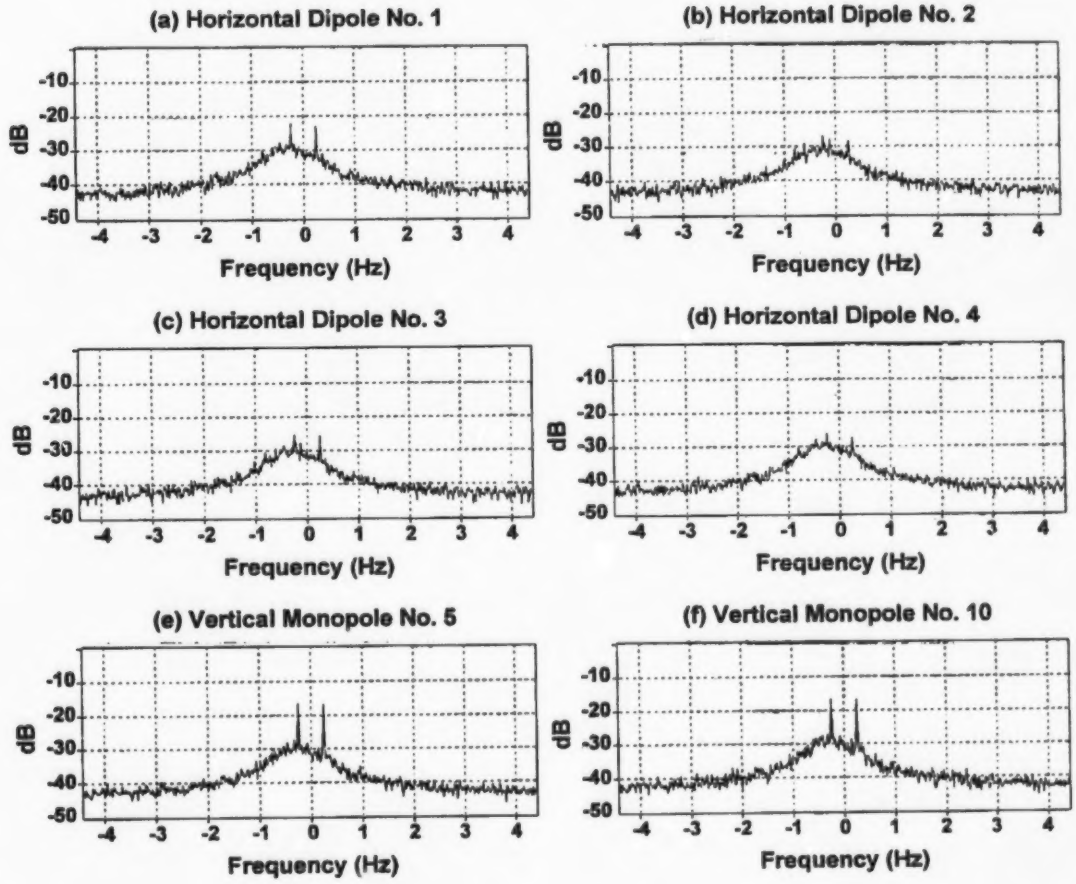

Figure 4 Power spectral densities of outputs from auxiliary antennas at the specified range bin of 15; (a)-(d) -- horizontal dipoles; (e)-(f) -- vertical monopoles

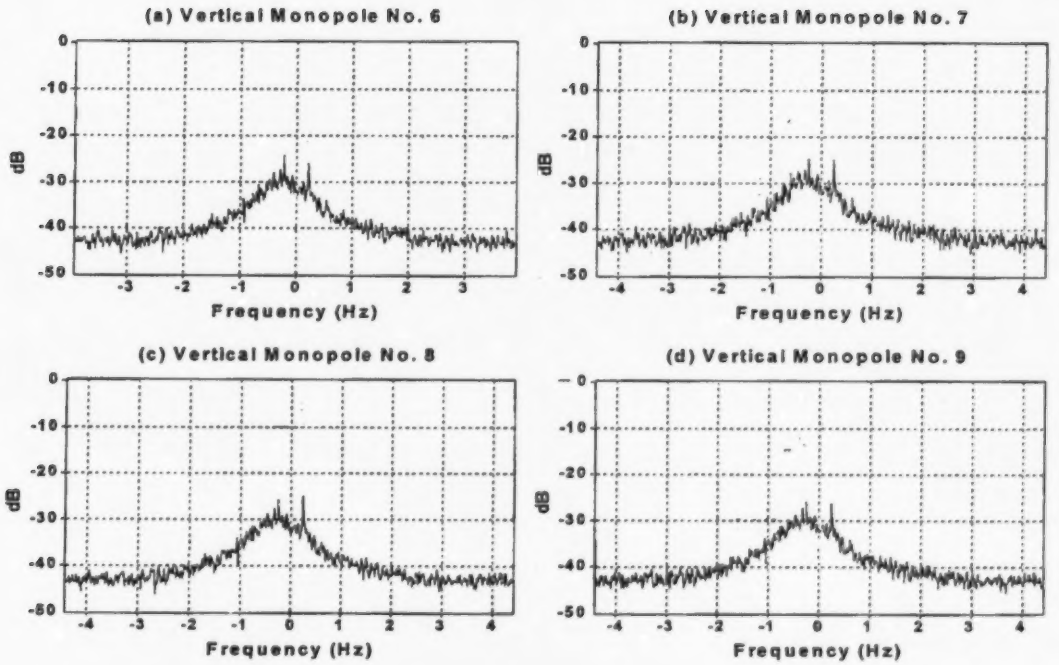

Figure 5 Power spectral densities of outputs from main antennas (vertical monopoles 6, 7, 8 and 9) at the specified range bin of 27

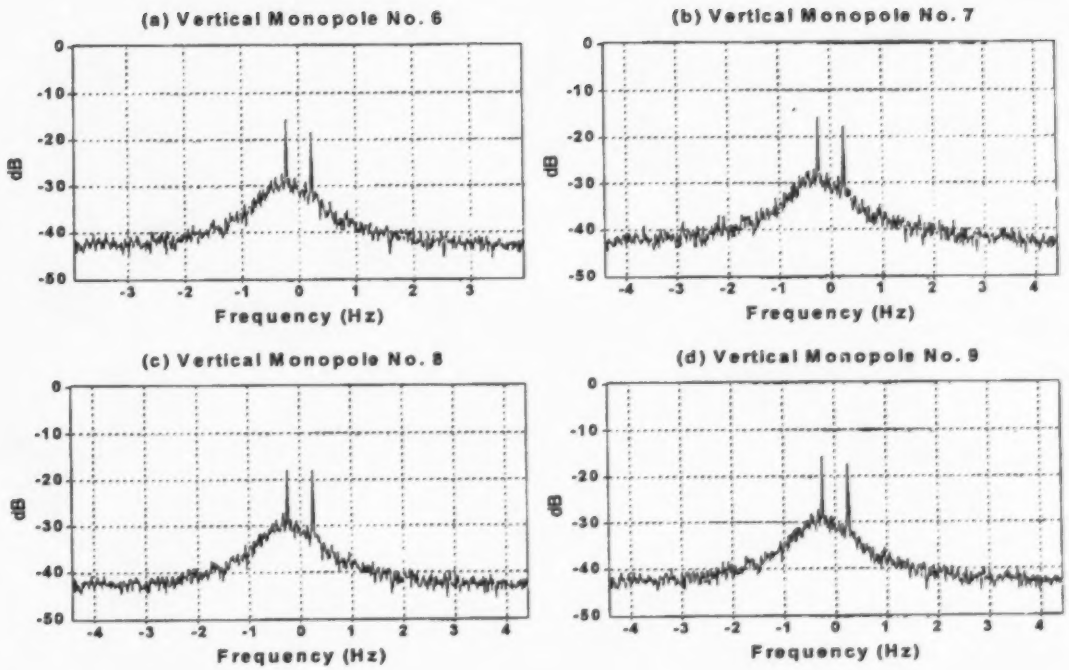

Figure 6 Power spectral densities of outputs from main antennas (vertical monopoles 6, 7, 8 and 9) at the specified range bin of 15

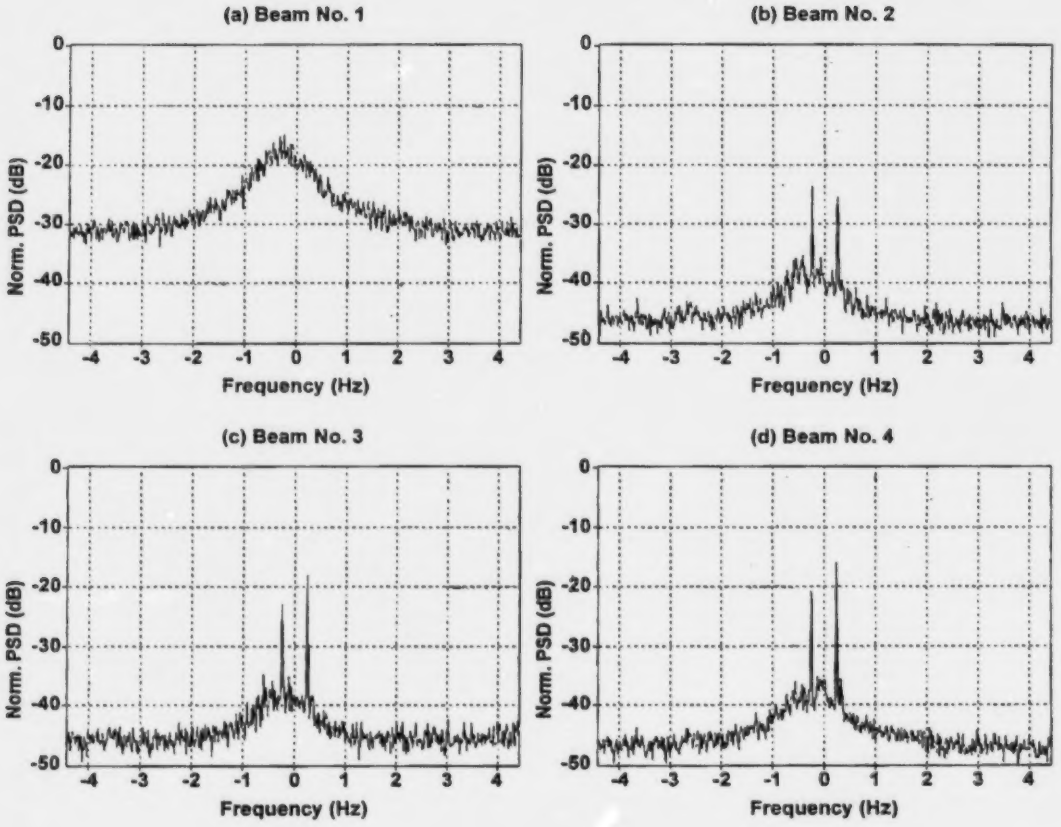

Figure 7 Power spectral densities of beamformed outputs from main array at the specified range bin of 27

4. Results of Interference Suppression

No real target signal is known to exist in the radar data. To gauge the effectiveness of the adaptive techniques before and after interference suppression, we inject a target signal at the outputs of the antenna array before the interference suppression. In the phases of the target signal, we take into account the locations of all antenna elements, including those of the horizontal dipoles. In the amplitudes of the target signal, we assume that (i) the amplitudes of the target signal are the same in the outputs of all the vertical antennas, and (ii) the amplitudes of the target signal in the horizontal antennas are half of the amplitude in the vertical antennas. Note that the second assumption is based on the observation made earlier on the powers of the Bragg lines in the outputs of the horizontal and vertical antennas, i.e., at range bin 15, the signal powers of the Bragg lines in the outputs of the horizontal antennas were about 6-8 dB lower than the signal powers of the Bragg lines in the outputs of the vertical antennas.

The target's azimuth, θ_t, and the target's Doppler frequency bin, l_t need to be specified before the target signal can be synthesised. Here, we consider the case when the target signal is coming from the same direction as the interfering signal. Target detection in HFSWR is normally carried out in the Doppler-frequency domain. The Doppler spectrum of the HFSWR data includes a sea-clutter continuum and a noise power spectrum. Sea clutter is normally confined in a small interval centred at 0 Hz, and is dominant over noise in the Doppler spectrum. Slow targets such as ships have Doppler frequencies inside the sea-clutter frequency band, and therefore, slow targets are detected against sea clutter. Fast targets such as aircraft have Doppler frequencies outside the sea-clutter frequency band, and therefore, fast targets are detected against noise. In this section, we also evaluate the effectiveness of the adaptive techniques on a slow target and a fast target, particularly when the target signal is coming from the same direction as the interfering signal.

4.1 Target signal coming from the same direction as the interfering signal

The interfering signal was coming from the boresight direction of the main antenna array. Figure 8(a) shows the Doppler spectrum of the data obtained from the beam at the boresight direction of the array from range bin 27. The injected target signal has a Doppler frequency of 2 Hz, which corresponds to a radial velocity of -186 km/hour. This is a relatively fast target. This target signal is coming from the same direction as the interfering signal, and the signal strength of the target is at about 5 dB above the interference-plus-noise level at the target Doppler bin. Figure 8(b) shows the power Doppler spectrum of the data after interference suppression using the SLC technique with auxiliary horizontal dipoles 1 and 2. From Figure 8(b), one can observe that the interference is suppressed while the target signal is preserved. The signal power of the target is now at about 15 dB above the interference-plus-noise power level at the target Doppler bin. Figure 8(c) shows the power Doppler spectrum of the data after interference suppression using the SLC technique with auxiliary horizontal dipoles 3 and 4. Here, one can also observe that the interference is suppressed while the target signal is preserved. The signal power of the target is also at about 15 dB above the interference-plus-noise power level. Figure 8(d) shows the power Doppler spectrum of the data after interference suppression using the SLC technique with auxiliary vertical monopoles 5 and 10. One can observe that both the interfering signal and the target signal are cancelled.

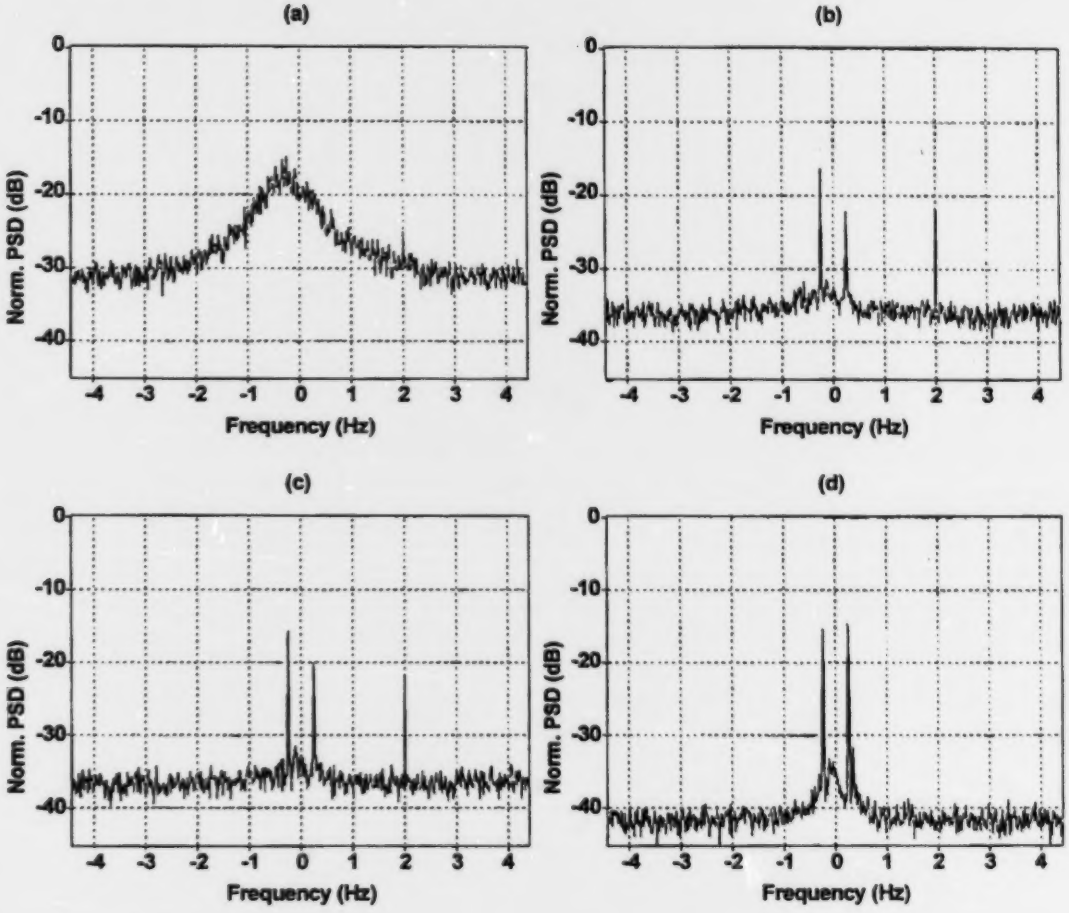

Figure 8 Power spectral densities before interference Suppression (a), after interference suppression with auxiliary horizontal dipoles 1 and 2 (b), after interference suppression with auxiliary horizontal dipoles 3 and 4 (c), and after interference suppression with auxiliary vertical monopoles 5 and 10 (d); The target Doppler frequency is at 2 Hz.

It should be pointed out that in Figure 8(d), there is a false target signal at the Doppler frequency of 0.334 Hz, whereas in Figures 8(b) and 8(c), this false target signal is not present. The presence of the false target signal in Figure 8(d) is due to a stronger contribution of the second-order sea clutter [3] from the outputs of the auxiliary vertical antennas. This stronger contribution of the sea clutter is further enhanced in Figure 8(d) because of a lower interference-plus-noise power level in the Doppler spectrum. As shown in Figure 8(d), the noise floor is more than 4 dB lower than those in Figures 8(b) and 8(c). More discussion of the effects of the adaptive SLC techniques on the interference-plus-noise levels will be presented in Section 4.3.

The change in the target signal is even more dramatic when we have a slow target signal. Figure 9(a) shows the Doppler spectrum of the same data obtained from the beam at the boresight direction of the main array. The injected target signal now has a Doppler frequency of –0.132 Hz, which corresponds to a radial velocity of 12.3 km/hour. This signal has the same strength as the fast target signal discussed above, but the slow target is not observable in Figure 9(a) because of the interference. Figures 9(b) and 9(c) show the Doppler spectra of the data after interference suppression with the two horizontal dipole pairs. The interference is now cancelled and the target signal is clearly observable at the specified Doppler frequency of –0.132 Hz. As shown in Figures 9(b) and 9(c), the power of this target signal is at about 12 dB above the residual interference-plus-noise power level. Figure 9(d) shows the Doppler spectrum of the data after interference cancellation using the vertical monopole antennas. Again, both the interfering and the target signals are cancelled in this latter case.

Note that the false target signal at the Doppler frequency of 0.334 Hz is also present in Figure 9(d). This false target signal, however, is not present in Figures 9(b) and 9(c). As explained earlier, the presence of this false target signal in Figure 9(d) is due to a stronger contribution of the second-order sea clutter from the outputs of the auxiliary antennas, enhanced by a lower interference-plus-noise floor in Figure 8(d).

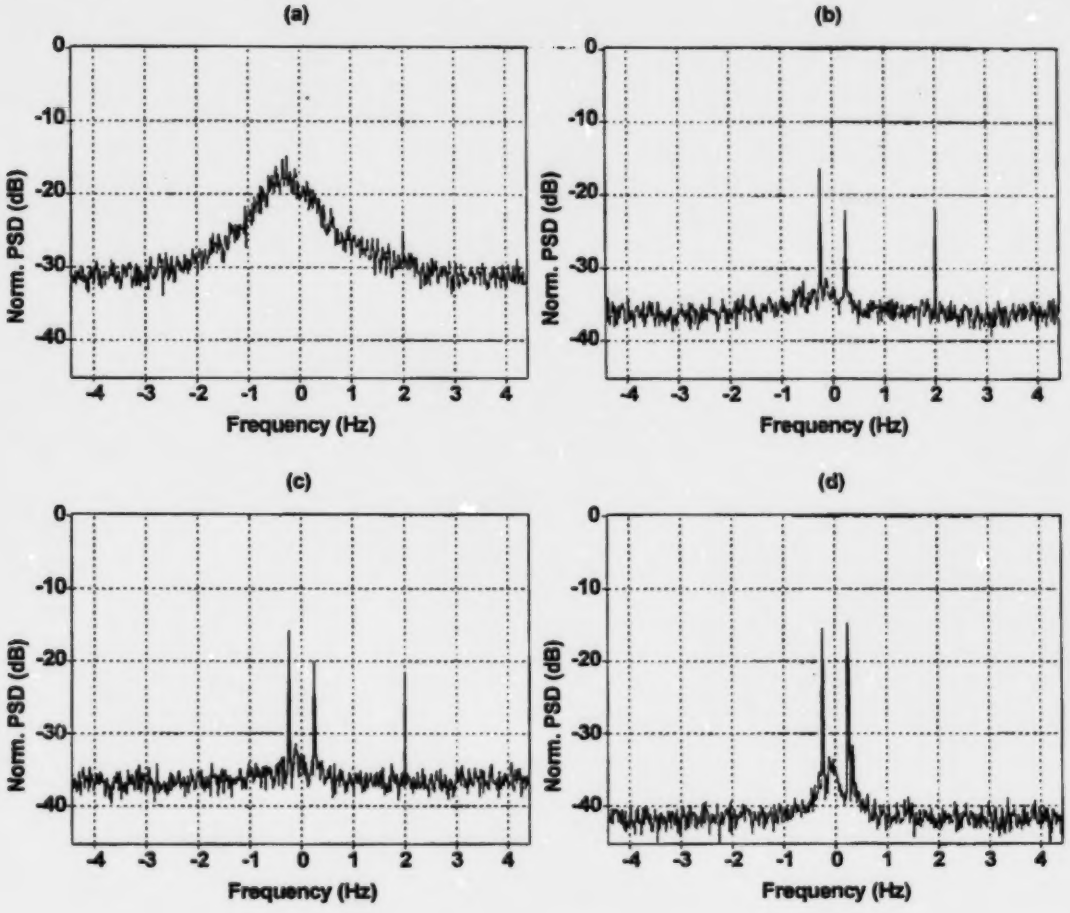

Figure 9 Power spectral densities before interference Suppression (a), after interference suppression with auxiliary horizontal dipoles 1 and 2 (b), after interference suppression with auxiliary horizontal dipoles 3 and 4 (c), and after interference suppression with auxiliary vertical monopoles 5 and 10 (d); The target Doppler frequency is at –0.132 Hz.

The two sets of results above are not totally unexpected. The cancellation of the target signal is expected when the vertical monopoles are used as auxiliary antennas. The adaptive technique simply forms a null in the direction of the interfering signal, which also cancels the target signal. The preservation of the target signal is expected in theory when we use the horizontal dipoles as auxiliary antennas. This is because the horizontal antennas are not expected to receive the vertically polarized target signal. In practice, however, the horizontal dipoles could receive the target signals, often due to the sagging or mis-alignment of the horizontal antennas. The results here show that the target signal is not cancelled, despite the fact that there is the presence of the radar signal in the output of the horizontal antennas.

4.2 Effects of Interference Suppression on Sea Clutter and Interference-plus-Noise Power Spectral Densities

We then look at the effects of the techniques on the sea clutter and interference-plus-noise power densities. We can do that by superimposing plots of the spectral power densities before and after the interference suppression. Figure 10 shows the superimposed spectra of the outputs from the beam at the boresight of the main array (Beam No. 1). Here, we show only one of the two spectra obtained by using the auxiliary horizontal antennas since they have similar background interference-plus-noise levels. We can clearly observe from Figure 10 that the interference-plus-noise level, or simply called the noise floor, is further lowered when we use the vertical monopoles as auxiliary antennas. The adaptive technique uses the correlation between the outputs of the main and auxiliary antennas to estimate the interference components in the outputs of the main antennas. The difference in the noise floor is likely due to the fact that the interference components received by the vertical antennas are better correlated than those received by the horizontal and vertical antennas. From Figure 10, we can also observe that the Bragg lines are slightly enhanced when the vertical monopoles are used as auxiliary antennas. This is likely due to an additional contribution of the sea clutter from the auxiliary vertical antennas.

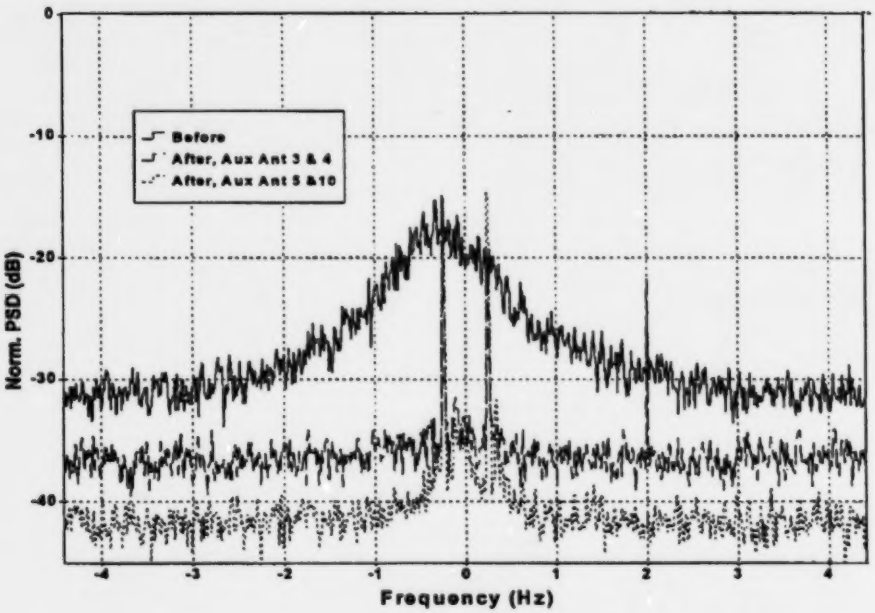

Figure 10 Superimposed Doppler spectra of outputs from beam no. 1 before and after interference suppression

Similarly, Figures 11-13 show the superimposed spectra of the outputs from beams No. 2, 3 and 4. However, the noise floors in Figure 11-13 do not seem to change much before and after interference suppression. While the interference in the Doppler interval approximately between -1.5 and 1 Hz is suppressed by using the auxiliary antennas, the noise floors beyond this interval are essentially the same before and after interference suppression. The results here are actually not surprising. The SLC techniques cancel the interference components only, and the techniques cannot cancel the white background noise. Figures 11-13 essentially show that power levels outside the Doppler interval of –1.5 and 1 Hz are at the background levels.

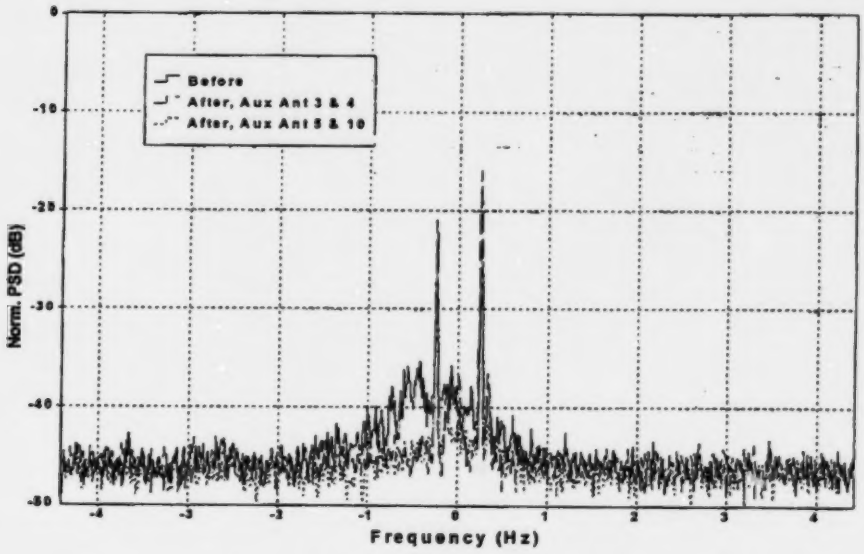

Figure 11 Superimposed Doppler spectra of outputs from beam no. 2 before and after interference suppression

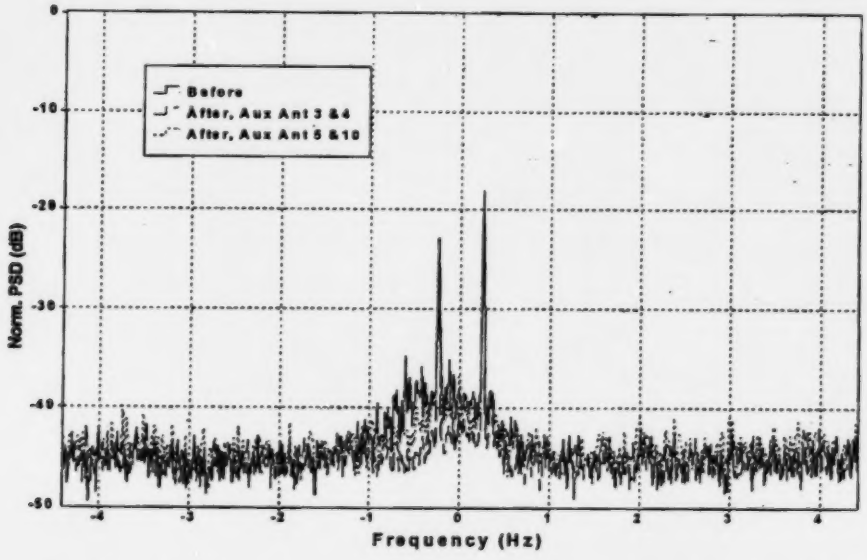

Figure 12 Superimposed Doppler spectra of outputs from beam no. 3 before and after interference suppression

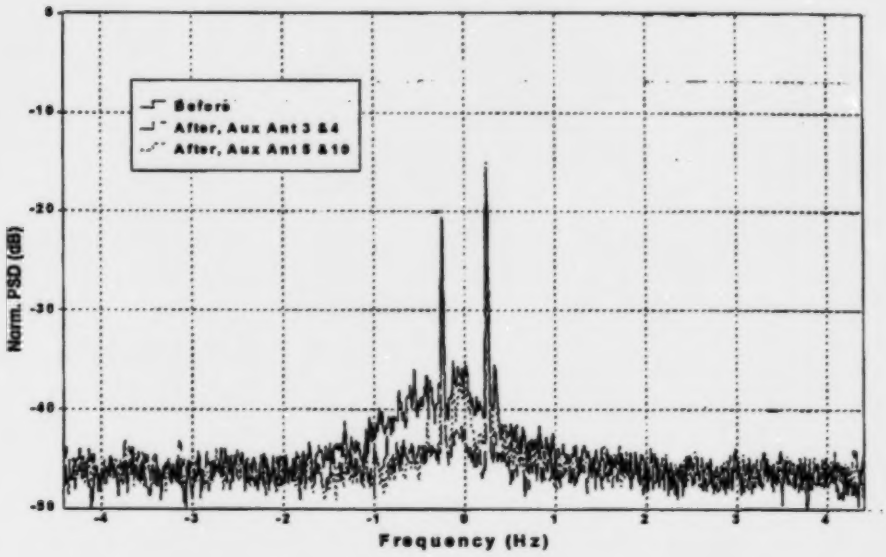

Figure 13 Superimposed Doppler spectra of outputs from beam no. 4 before and after interference suppression

4.3 Implications of Experimental Results

The results above show that the adaptive SLC technique using auxiliary vertical monopoles fails when the target signal is coming from the same direction as the interfering signal. This failure may have grave consequences in HFSWR operations. It could lead to a failure to detect targets close to the interference direction.

The results also show that the adaptive technique using the horizontal dipoles as auxiliary antennas does not suppress the target signal, even when it is coming from the same direction as the interfering signal. This is possible in spite of the fact that the dipoles received some radar signals during the experiment. Hence, this technique using the auxiliary horizontal dipoles could aid the radar to provide an unobstructed coverage.

5. Conclusions and Recommendations

For a target signal coming from the same direction as the interfering signal, we found that both the interfering and the target signals were cancelled when the vertical monopoles were used as auxiliary antennas. However, the target signal was preserved while the interference was cancelled when the horizontal dipoles were used as auxiliary antennas. This latter result was obtained in spite of the fact that the horizontal dipole antennas received some radar signals.

The cancellation of targets from the same direction as the interfering signal, when auxiliary vertical antennas were used, could lead to a failure to detect targets close to the interference direction. This failure, however, could be avoided if we used horizontal antennas such as horizontal dipoles as auxiliary antennas in the SLC system.

The results above were obtained using a synthetic target signal injected into measured radar data. To further verify the results above, it is recommended that we carry out a similar experiment with a real target signal in the radar data.

Due to the fact that the interference components received by similar antennas are more correlated than those received by different antennas, the interference could be suppressed more substantially when we use the vertical antennas. Our results showed that the interference-plus-noise floor could be further lowered when the vertical monopoles were used as auxiliary antennas. However, the best the SLC techniques could do was to lower the interference-plus-noise floor to the background noise levels.

Acknowledgements

The author would like to thank Northern Radar Systems Limited (NRSL) for supplying the radar data. NRSL carried out the radar experiment under contract to Defence Research Establishment Ottawa, Canada.

Reference

1. Howells, "Intermediate Frequency Sidelobe Canceller", U.S. Patent 3 202 990, August, 1965.
2. S. P. Aplebaum, "Adaptive Arrays", IEEE Transactions on Antennas and Propagation, AP-24, September 1976, pp.585-598.
3. Widrow B, Glover J, McCool J, Kaunitz J, Williams C, Hearn R, Zeidler J, Dong E and Goodlin R, "Adaptive Noise Cancelling: Principles and Applications", Proceedings of IEEE, Vol. 63, No. 12, December 1975, p. 1692.
4. D.E. Barrick, "Remote Sensing of Sea State by Radar", Chapter 12, in "Remote Sensing of troposphere", Edited by V. Derr, GPO, Washington, DC, 1972.
5. F. J. Harris, "On the Use of Windows for Harmonic Analysis with the Discrete Fourier Transform", Proceedings of the IEEE, Vol. 66, No. 1, January 1966, pp. 51-83.